Separation Science and Technology
Publication details, including instructions for authors and subscription information:
http://www.informaworld.com/smpp/title~content=t713708471

Polyetherimide Hollow-Fiber Module for the Removal of Volatile Organic Compounds from Air: Experimental Results and Computer Simulation

S. Deng[a]; K. Lang[a]; T. Matsuura[a]; A. Tremblay[a]
[a] DEPARTMENT OF CHEMICAL ENGINEERING, INDUSTRIAL MEMBRANE RESEARCH INSTITUTE, UNIVERSITY OF OTTAWA, OTTAWA, CANADA

Online publication date: 11 September 2000

To cite this Article Deng, S. , Lang, K. , Matsuura, T. and Tremblay, A.(2000) 'Polyetherimide Hollow-Fiber Module for the Removal of Volatile Organic Compounds from Air: Experimental Results and Computer Simulation', Separation Science and Technology, 35: 14, 2227 — 2242
To link to this Article: DOI: 10.1081/SS-100102099
URL: http://dx.doi.org/10.1081/SS-100102099

SEPARATION SCIENCE AND TECHNOLOGY, **35**(14), pp. 2227–2242, 2000

Polyetherimide Hollow-Fiber Module for the Removal of Volatile Organic Compounds from Air: Experimental Results and Computer Simulation

S. DENG, K. LANG, T. MATSUURA*, and A. TREMBLAY
INDUSTRIAL MEMBRANE RESEARCH INSTITUTE
DEPARTMENT OF CHEMICAL ENGINEERING
UNIVERSITY OF OTTAWA
OTTAWA, CANADA, K1N 6N5

ABSTRACT

A hollow-fiber module with an effective area of 1705 cm^2 was constructed and tested for the removal of acetone from air. Hollow fibers were made of polyetherimide and used without silicone rubber coating. It was found that acetone could be effectively removed when the residence time of the nitrogen stream in the module was sufficiently long. A set of equations was used for computer simulation of the module. The calculated values agreed very well with the experimental ones.

Key Words. Hollow-fiber module; Computer simulation; Vapor permeation; Polyetherimide membrane; Removal of volatile organic compounds

INTRODUCTION

In recent years air pollution has become most serious, especially in technologically advanced countries. In these countries, many industrial processes handling organic solvents produce solvent-containing exhaust streams. Theses streams cause not only severe air pollution problems but also significant economic loss. From an environmental point of view, it is necessary to limit and control organic vapor emissions because they affect the composition of

* To whom correspondence should be addressed.

the ozone layer, climate change, the growth and decay of plants, and the health of human beings and all species of animals.

Two types of conventional organic emission-control techniques still in use (1, 2) are processes to recover organic vapors, including adsorption, absorption, and condensation; and processes to destroy organic vapors, including direct flame incineration, thermal incineration, and catalytic incineration. Each technique has advantages and disadvantages, in regard to safety, performance, operating costs, and facility space.

In recent decades significant achievements have been made in many areas of membrane technology. The separation of organic vapors by a membrane process may have great economic potential (3, 4). For example, Chmiel et al. reported on a process in which adsorption and membrane separation are coupled to remove VOCs from exhaust gas (5). The concentration of a component, (1-methoxy-propyl)-acetate, of a solvent in the desorbate stream by a membrane module was demonstrated. In stripping air from the soil the hydrocarbons were adsorbed; the desorbed vapor was then concentrated by a membrane process (6). Other attempts were made to explore the possibility of membrane processes to remove VOCs from air (3, 4, 7–12). Most of the published research on organic vapor permeation by membranes was performed using composite silicone rubber membranes supported on a porous polymer substrate. Polysulfone membranes were usually used as a substrate. The resistance of silicone rubber to hydrocarbons and gasoline is however poor (11). Therefore, attempts were made to use some glassy polymers without coating. Ilinitch et al. (12) used polyphenylene oxide (PPO) and some PPO-based copolymer membranes for separation of hydrocarbons. Aromatic polyimide (PI) and polyetherimide (PEI) were employed for the preparation of membranes to remove various organic vapors from nitrogen by Feng et al. (13, 14) and Deng et al. (15–19). The molecular structure of organic vapors and the selectivity data were correlated. A strong correlation was found between the chromatographic retention time of organic vapors and their selectivity. These experimental results led to the conclusion that sorption was the factor governing the separation of organic compounds from nitrogen. Furthermore, a membrane was prepared by coating the surface of a porous polyetherimide membrane with silicone rubber. The performance of membranes with and without silicone rubber coating was compared (16). Attempts were made to find appropriate conditions to spin high-performance hollow fibers for the removal of organic vapors from nitrogen and air. Hollow fibers were also prepared with and without silicone rubber coating at the internal wall, and their performance was compared. The effect of the presence of water in the feed stream was also studied (17). The system designs were attempted for vapor–gas separation systems (20). Membrane separation and absorption-stripping were combined in a hybrid system for VOC removal (21). Water-alcohol separation

in the vapor phase was also attempted by using polyetherimide (22) and sodium alginate membranes (23).

The objective of this work was to construct a prototype hollow-fiber module to investigate its performance for the removal of organic vapors from nitrogen. For this purpose, the hollow fibers spun in previous work (18) were used. A computer simulation of the hollow-fiber module was also attempted, and the calculated values were compared with the experimental ones.

EXPERIMENTAL

Hollow-Fiber Preparation

The composition of the polymer solution used for hollow-fiber spinning and hollow-fiber spinning conditions are summarized in Table 1. The dimensions of hollow fibers are also included in Table 1. The selective skin layer of the hollow fiber was formed on the bore side of the hollow fiber.

Module Construction

A hollow-fiber module with an effective area of 1705 cm^2 was constructed. The structure of the module is schematically shown in Fig. 1. A bundle of 300

TABLE 1
Hollow-Fiber Spinning Conditions and Hollow-Fiber Dimensions

Composition of spinning solution, wt%	
Polyetherimide	29.0
$LiNO_3$	1.0
Dimethyl acetamide	66.7
Acetone	3.3
Hollow-fiber spinning conditions	
Solution temperature	27°C
Pressure applied on polymer solution	20 psig
Air gap	80 cm
Internal coagulant	aqueous glycerol solution
Temperature of internal coagulant	23°C
Flow rate of internal coagulant	7.5 mL/min
External coagulant	water
Temperature of external coagulant	17.5°C
Hollow-fiber dimensions	
Inside diameter	0.75 mm
Outside diameter	1.25 mm
Wall thickness	0.25 mm

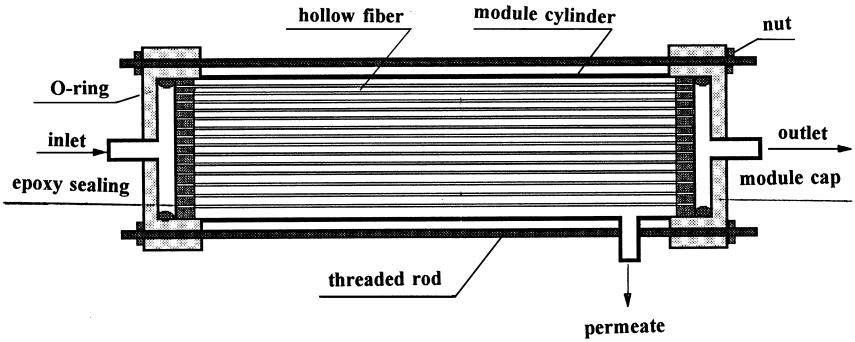

FIG. 1 Schematic diagram of hollow-fiber module.

28-cm long hollow fibers was installed in a 5-cm diameter plastic cylinder. Epoxy resin (Canus CAN) was applied up to 2 cm from both ends of the hollow-fiber bundle to fill the space between hollow fibers and that between the hollow-fiber bundle and the internal wall of the cylinder. The application method is as follows: The mixture of 4 : 1 : 0.4–0.67 (epoxy resin : epoxy hardner : ethanol by weight) was injected into both ends of the module after they were capped. The center of the module was then connected to a motor shaft and the module was rotated around its central axis overnight. Epoxy was driven into the ends of the module by centrifugal force. After hardening of the resin, the caps were removed and the excess resin was cut off. To test the sealing with epoxy resin, pressurized air (20 psig) was supplied to the shell side of the module, while the entire module was immersed in water. No air bubble formation was observed, ensuring perfect sealing.

The module was then connected to the vapor-permeation system described earlier (18). It should be noted that the feed gas–vapor mixtures were introduced to the bore side of the hollow fiber. Therefore, the bore side and the shell side of the hollow fiber are hereafter called feed side and permeate side, respectively.

Vapor Permeation

Nitrogen gas was introduced to the feed side, while vacuum was applied on the permeate side for 1 d to remove residual solvent in the hollow fiber completely. Then nitrogen permeability was measured, which was followed by the permeation experiments of feed acetone–nitrogen mixtures. The details of the permeation experiments were reported elsewhere (17). The variables in the experiments were acetone mole fraction at the module inlet, pressure on the permeate side, and the flow rate of the feed stream at the module inlet. The

pressure at the module outlet was kept atmospheric, and the temperature was ambient throughout the experiments.

THEORETICAL

A set of equations that describe the steady-state operation of the hollow-fiber module was established according to the schematic diagram illustrated in Fig. 2. The following assumptions were made:

1. The permeances are independent of the composition.
2. The pressure drop on the permeate side is negligible and equal to the permeate outlet pressure p_3^L.
3. The pressure drop of the feed stream is governed by the Hagen-Poiseuille law.

Under the above assumptions, change in the flow velocity of the feed stream is given by

$$-\frac{du_1(x)}{dx} = \frac{4d_e}{d_i^2}[Q_A(x) + Q_N(x)] \tag{1}$$

Change in the acetone mole fraction in the feed is given by

$$-\frac{dX_{A1}(x)}{dx} = \frac{4d_e}{u_1(x)d_i^2}[Q_A(x)X_{N1}(x) - Q_N(x)X_{A1}(x)] \tag{2}$$

Pressure drop of the feed stream is given by

$$-\frac{d[p_1(x)]^2}{dx} = \frac{64\mu RT}{d_i^2}u_1(x) \tag{3}$$

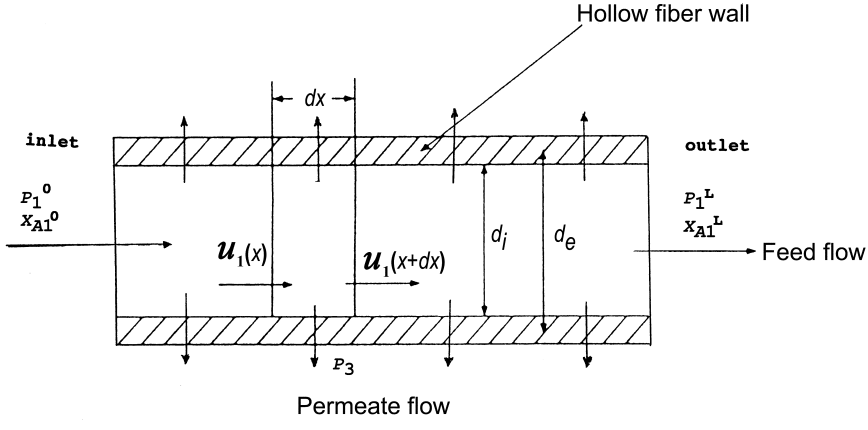

FIG. 2 Mass transport in a hollow fiber.

From mass balance

$$S_1 u_1(x) + S_3 u_3(x) = S_1 u_1^0 \tag{4}$$

From material balance

$$S_1 u_1(x) X_{A1}(x) + S_3 u_3(x) \overline{X_{A3}} = S_1 u_1^0 X_{A1}^0 \tag{5}$$

Equations for mole fractions are

$$X_{A1}(x) + X_{N1}(x) = 1 \tag{6}$$

$$\overline{X_{A3}}(x) + \overline{X_{N3}}(x) = 1 \tag{7}$$

$$X_{A3}(x) + X_{N3}(x) = 1 \tag{8}$$

The flux for acetone vapor (A) and nitrogen gas (N) are given by

$$Q_A(x) = J_A [p1(x) X_{A1}(x) - p_3 X_{A3}(x)] \tag{9}$$

$$Q_N(x) = J_N [p_1(x) X_{N1}(x) - p_3 X_{N3}(x)] \tag{10}$$

$$X_{A3}(x) = \frac{Q_A(x)}{Q_A(x) + Q_N(x)} \tag{11}$$

Equations (1) to (11) are solved under the boundary conditions (12) to (16). All symbols are defined in the Nomenclature section.

$$u_1(0) = u_1^0 \tag{12}$$

$$X_{A1}(0) = X_{A1}^0 \tag{13}$$

$$p_1(0) = p_1^0 \tag{14}$$

$$u_3(0) = 0 \tag{15}$$

$$\overline{X_{A3}}(0) = X_{A3}(0) \tag{16}$$

RESULTS AND DISCUSSION

Vapor Permeation Experiments

Results of permeation experiments are summarized in Table 2. The acetone mole fraction decreased from 0.309 at the module inlet to 0.031 at the module outlet in experiment U1. Hence, acetone recovery to the permeate was 90%. Considering the short fiber length, the acetone recovery seems quite satisfactory.

Looking into the data from experiments C1 to C5, the acetone mole fraction at the feed inlet, X_A^0, was increased from 0.052 to 0.327, while the permeate

TABLE 2
Experimental Results for Different Conditions

No.	X_A^0	P_3^a (mm Hg)	u_i^{0b} (mL/min)	X_A^L	PR^c (mol/s)	u_1^{Lb} (mL/min)
C1	0.052	1.4	112.9	0.051	1.72E-6	107.9
C2	0.119	1.4	112.8	0.078	3.80E-6	105.3
C3	0.180	1.45	106.3	0.116	5.90E-6	98.2
C4	0.250	1.45	108.6	0.150	7.67E-6	103.1
C5	0.327	1.45	108.4	0.166	9.26E-6	101.7
P1	0.320	1.4	76.1	0.165	1.21E-5	68.9
P2	0.330	4.0	76.1	0.160	1.20E-5	69.2
P3	0.331	9.4	76.2	0.169	1.27E-5	69.8
P4	0.337	14.4	76.4	0.178	1.22E-5	69.5
P5	0.337	19.3	76.6	0.179	1.22E-5	70.3
U1	0.309	1.4	20.0	0.031	7.47E-6	18.9
U2	0.319	1.4	35.1	0.067	1.06E-5	32.5
U3	0.322	1.45	63.2	0.139	1.32E-5	59.5
U4	0.349	1.45	76.0	0.165	1.45E-5	72.5
U5	0.358	1.45	92.8	0.185	1.57E-5	89.1

Note: 1. The membrane operation temperature was room temperature, 24.5°C.
2. The inlet feed pressure (P_1) was atmosphere pressure.
[a]1 mm Hg = 133.32 Pa.
[b]1 mL/min = 0.00556 mol/s·m^2 for the cross sectional area of 1.339×10^{-4} m^2.
[c]*PR* is overall acetone permeation rate.

pressure, p_3, and feed flow velocity, u_1^0, were kept constant. The acetone mole fraction at the feed outlet, X_A^L, and the overall acetone permeation rate through the entire membrane area (*PR*) increased as X_A^0 increased.

In the next series, experiments P1 to P5, the permeate pressure p_3 was increased while X_A^0 and u_1^0 were kept constant. X_A^L and *PR* were practically unaffected throughout the series, because partial vapor pressure of acetone in the feed was about $0.33 \times 760 = 251$ mm Hg, which was far above the maximum permeate pressure of 19.3 mm Hg. Thus, the driving force for the acetone permeation was practically governed by the partial pressure of acetone in the feed. In the last series of experiments, U1 to U5, u_1^0 was increased from 20.0 to 92.8 mL/min, while X_A^0 and p_3 were kept constant. The acetone concentration in the feed outlet, X_A^L, increased from 0.031 to 0.185, and *PR* increased from 7.47×10^{-6} mol/s to 1.57×10^{-5} mol/s. Increase in X_A^L is natural because the residence time of the feed mixture in the module decreased. The increase in *PR* is due to an increase in the average feed acetone mole fraction in the module.

Comparison of Experimental and Calculated Values

The permeance data used for the computer simulation were 2.80×10^{-9} and 2.66×10^{-11} mol/s·m^2 Pa, respectively, for acetone and nitrogen. These values were obtained in earlier work (18) using a laboratory-scale hollow-fiber module, the effective area of which was 140 cm^2. The saturation vapor pressure of acetone at 24.5°C (the operating temperature) is 52.39 kP, corresponding to a mole fraction of 0.517 when the total pressure is 1 atmospheric pressure. Considering the feed mole fraction of 0.052 to 0.358, in most cases above 0.3, one might ask about the validity of the assumption of constant acetone permeance, because the latter mole fraction is close to that of the saturation vapor pressure. It should however be recalled that the acetone permeance was obtained in earlier work (18) with a feed acetone mole fraction of 0.3–0.33. This justifies the single permeance in our computer simulation. Also note that the feed pressure drop from the module inlet to the outlet was negligible both in experiment and in calculation, although the calculation of the pressure drop by the computer program was possible. Comparison of experimental and calculated values was made in Figs. 3–5 for overall acetone permeation rate throughout the entire membrane area in the module. Inlet acetone mole fraction, permeate pressure, and feed flow rate at the module inlet were the variables. Comparison of experimental and calculated values was made with respect to the acetone mole fraction at the module outlet in Figs. 6–8. All figures show that the calculated values represent the values obtained experimentally very well.

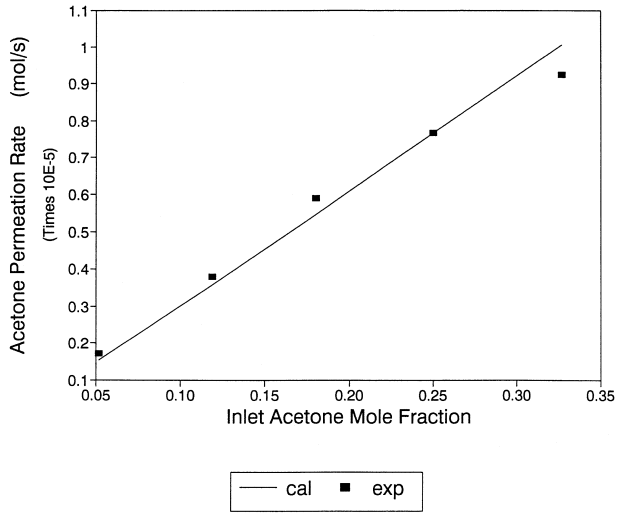

FIG. 3 Overall acetone permeation rate vs. inlet acetone mole fraction.

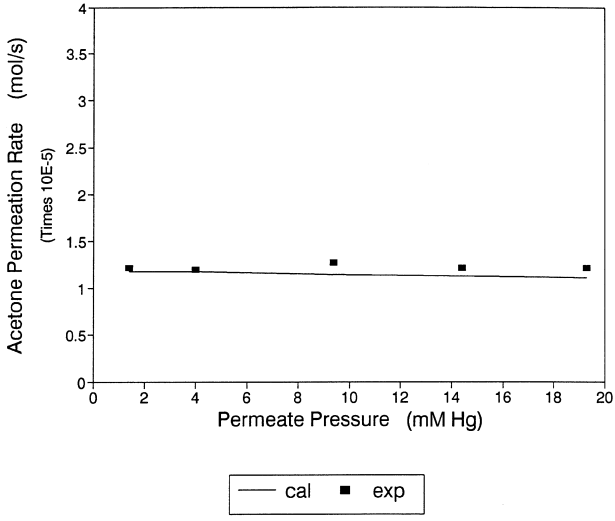

FIG. 4 Overall acetone permeation rate vs. permeate pressure.

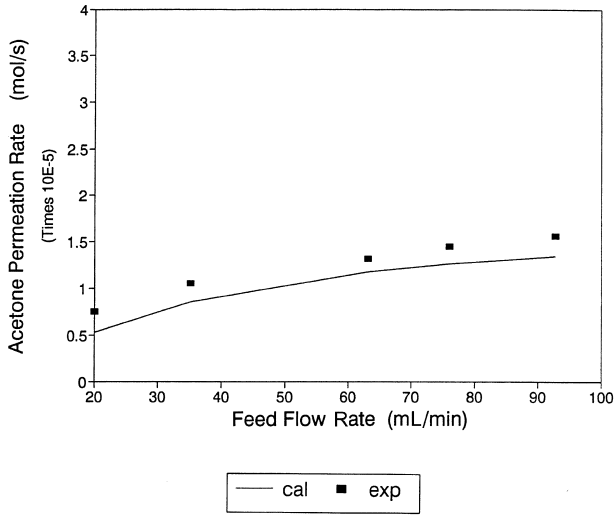

FIG. 5 Overall acetone permeation rate vs. feed flow rate.

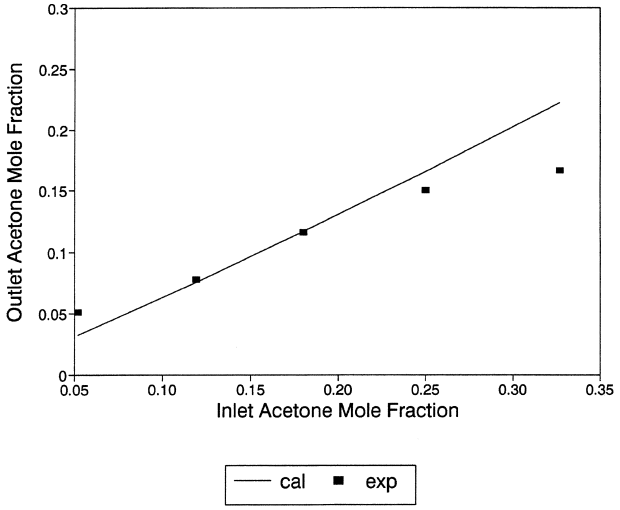

FIG. 6 Outlet acetone mole fraction vs. inlet acetone mole fraction.

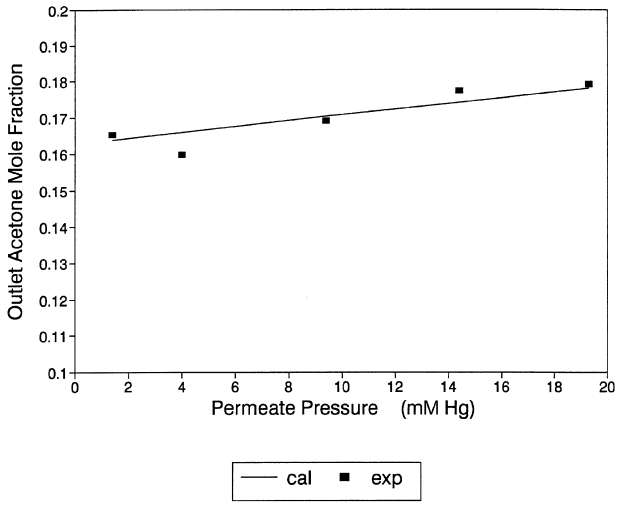

FIG. 7 Outlet acetone mole fraction vs. permeate pressure.

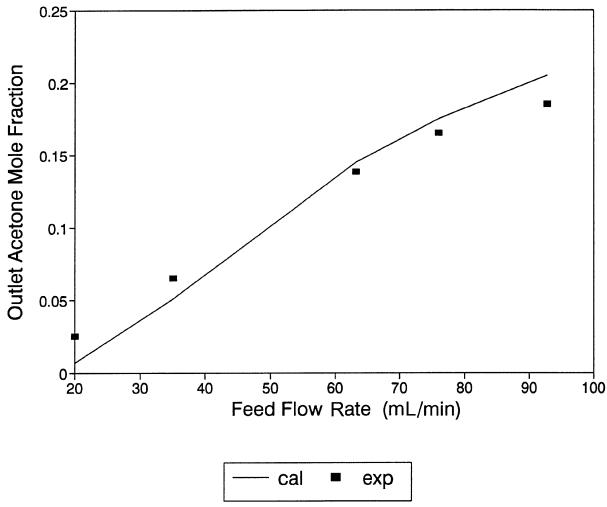

FIG. 8 Outlet mole fraction vs. feed flow rate.

Results from Computer Simulation

Computer simulation allows acquisition of data that are difficult to obtain experimentally. Results of two such simulations are shown in Figs. 9 and 10. Figure 9 illustrates the profile of the vapor mole fraction along the longitudinal direction of the module for different vapor permeances. The figure enables us to know the hollow-fiber length to achieve a preset level of vapor mole fraction in the module outlet. Figure 10 shows the vapor mole fraction in the permeate as a function of vapor permeance. The figure indicates that the mole fraction of organic vapor in the permeate is more than 0.9 when the permeance is more than 7×10^{-10} mol/s·m^2 Pa.

The effect of the temperature was also calculated using the following values for the activation energy of membrane permeation.

Nitrogen	17,870 J/mol
Acetone	−55,700 J/mol for 20–40°C and −14,647 J/mol for 40–60°C

The above data were obtained in earlier work (19). The negative activation energy of acetone is due to the greater energy of sorption of acetone to the membrane than the activation energy of diffusion through the membrane. The decrease in the absolute value of the activation energy at high temperatures is probably due to a decrease in the energy of sorption at higher temperatures. Figures 11 and 12 show the effect of temperature on the overall permeation rate of acetone through the entire membrane area in the module

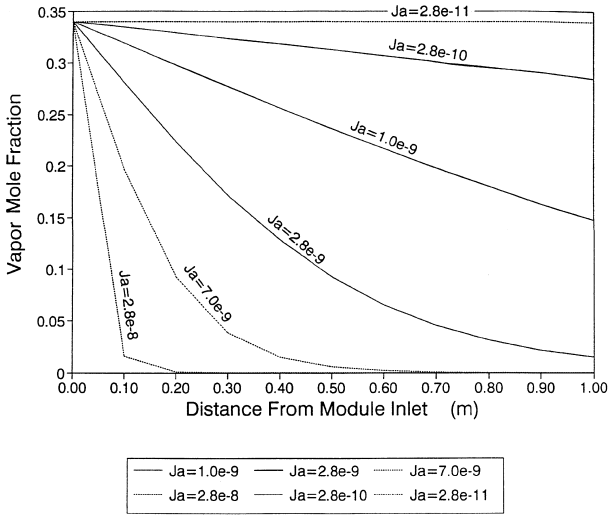

FIG. 9 Profile of vapor mole fraction in the module for different vapor permeances. Operating conditions: $p_1 = 760$ mm Hg, $p_3 = 1.4$ mm Hg, $T = 24.5°C$ $u_1^0 = 100$ mL/min, $X_A^0 = 0.337$, $J_N = 2.66 \times 10^{-11}$ mol/s · m^2 Pa.

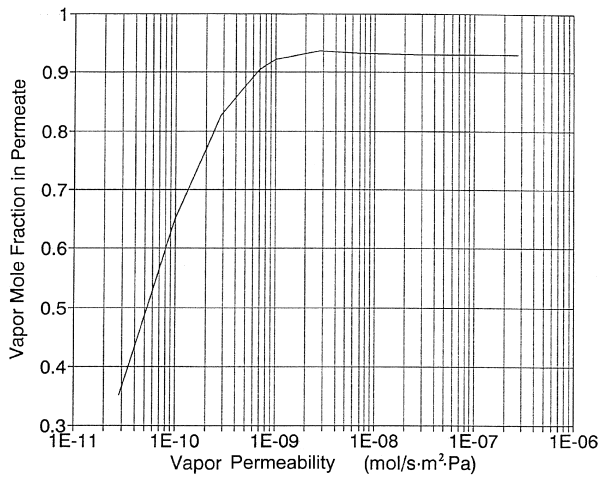

FIG. 10 Organic mole fraction at the permeate outlet for different permeances. Operating conditions: same as Fig. 9.

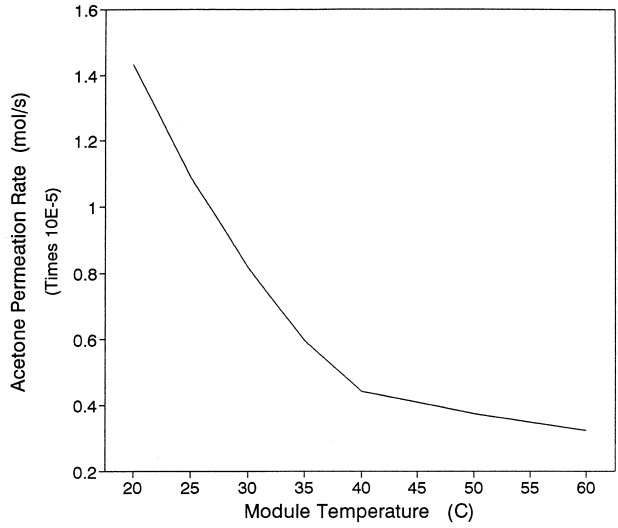

FIG. 11 Overall acetone permeation rate vs. operating temperature. Operating conditions: same as Fig. 9 except temperature.

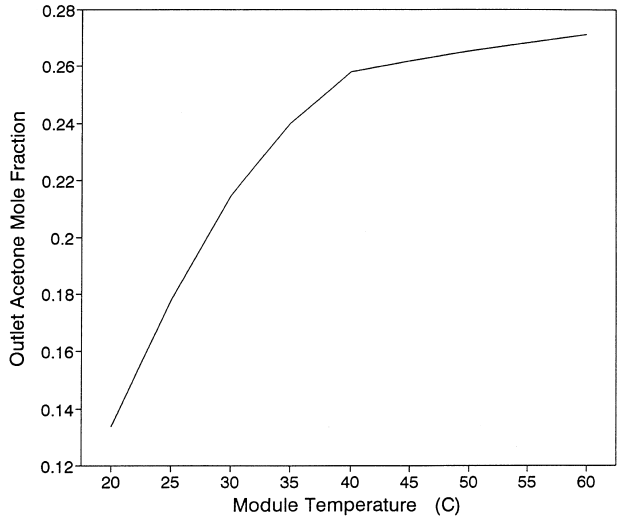

FIG. 12 Outlet acetone mole fraction vs. operating temperature. Operating conditions: same as Fig. 9 except temperature.

and on acetone mole fraction at the module outlet, respectively. Both figures indicate that the acetone recovery by the module decreases with an increase in temperature.

CONCLUSIONS

The following conclusions can be drawn from the above results.

1. A hollow-fiber module based on polyetherimide membrane is effective in the removal of volatile organic compounds from air.
2. A set of equations can simulate the hollow-fiber performance satisfactorily.
3. The computer simulation allowed acquisition of some module data that are difficult to obtain experimentally.

NOMENCLATURE

d_i	inside diameter of hollow fiber, m
d_e	effective diameter of hollow fiber, m
J	permeance, mol/s·m^2 Pa
L	length of hollow fiber, m
p	pressure, Pa
Q	permeate flux, mol/s·m^2
R	gas constant, 8.135 Pa m^3/mol K
S	cross sectional area, m^2
T	temperature
u	molar velocity, mol/s·m^2
x	distance from the module inlet
X	mole fraction
$\overline{X_3}$	average mol fraction of the permeate
μ	viscosity, Pa/s

Superscripts

0	module inlet
L	module outlet

Subscripts

A	acetone or organic vapor
N	nitrogen
1	feed
3	permeate

REFERENCES

1. K. Wark and C. F. Warner, "Air Pollution: Its Origin and Control," Harper & Row, New York, 1986.
2. L. Theodore and A. J. Buonicore, "Air Pollution Control Equipment," Vol. 2: Gasses, CRC Press, 1988.
3. R. D. Behling, "Separation of Hydrocarbons from Air," in *Proceedings of 6th Annual Membrane Technology Planning Conference*, Session V-4, Cambridge, 1986.
4. R. W. Baker, N. Yoshioka, J. M. Mohr, and A. J. Khan, "Separation of Organic Vapors from Air," *J. Membrane Sci.*, *31*, 259 (1987).
5. H. Chmiel, V. Mavrov, and M. Kaschek, "The Importance of Materials for Selective Separation in Production-Integrated Environmental Protection," in *Environmental Aspects in Materials Research*, (H. Warlimont, Ed.), DGM Informationsgesellschaft Verlag, 275–282, 1994.
6. H. Chmiel, V. Mavrov, and A. Fahnrich, "The Removal of VOCs from Exhaust Air and Vapor Condensates by Membrane Processes," in *Proceedings at the 1995 Thirteenth Annual Membrane Technology/Separations Planning Conference*, Newton, MA, Oct. 23–25, 1995.
7. K. V. Peinemann, J. M. Mohr, and R. W. Baker, "The Separation of Organic Vapors from Air," in *Recent Advances in Separation Technologies III, AIChE Symp. Ser., 82*, 250, 19 (1986).
8. K. Kimmerle, C. M. Bell, W. Gudernatch, and H. Chmiel, "Solvent Recovery from Air," *J. Membrane Sci., 36*, 577 (1988).
9. H. Paul, C. Philipsen, F. J. Gerner, and H. Strathmann, "Removal of Organic Vapor from Air by Selective Membrane Permeation," *Ibid., 36*, 363 (1988).
10. I. Pinnau, J. G. Wijmans, I. Blume, T. Kuroda, and K. V. Peinemann, "Gas Permeation through Composite Membranes," *Ibid., 37*, 81 (1988).
11. F. W. Billmeyer, Jr., *Textbook of Polymer Science*, 3rd ed., Wiley, New York, 1984.
12. O. M. Ilinitch, C. L. Semin, M. V. Chertova, and K. I. Zamaraev, "Novel Polymeric Membranes for Separation of Hydrocarbons," *J. Membrane Sci., 66*, 1 (1992).
13. X. Feng, S. Sourirajan, H. Tezel, and T. Matsuura, "Separation of Organic Vapors from Air by Aromatic Polyimide Membranes," *J. Appl. Polym. Sci., 43*, 1071 (1991).
14. X. Feng, S. Sourirajan, H. Tezel, and T. Matsuura, "Separation of Volatile Organic Compound/Nitrogen Mixtures by Polymeric Membranes," *Ind. Eng. Chem. Res., 32*, 533 (1993).
15. S. Deng, S. Sourirajan, T. Matsuura, and B. A. Farnand, "Volatile Hydrocarbon Emission Control by Polymeric Membranes," *Sixth International Conference on Pervaporation Processes in the Chemical Industry*, Ottawa, Sept. 27–30, 1992.
16. S. Deng, K. Lang, J. Wang, A. Tremblay, and T. Matsuura, "Membrane for the Removal of Volatile Organic Compounds from Air," *Memb. J. Korea, 7*, 22–30 (1997).
17. S. Deng, S. Sourirajan, T. Matsuura, and B. Farnand, "Study of Volatile Hydrocarbon Emission Control by an Aromatic Poly(etherimide) Membrane," *Ind. Eng. Chem. Res., 34*, 4494 (1995).
18. S. Deng, T. Liu, S. Sourirajan, T. Matsuura, and B. Farnand, "A Study of Volatile Hydrocarbon Emission Control by Polyetherimide Hollow Fiber Membranes," *J. Polymer Eng., 14*, 219 (1995).
19. S. Deng, A. Tremblay, and T. Matsuura, "Preparation of Hollow Fibers for the Removal of Volatile Organic Compounds from Air," *J. Appl. Polym. Sci., 69*, 371–379 (1998).
20. R. W. Baker, J. G. Wijmans, and J. H. Kaschemenkat, "The Design of Membrane Vapor–Gas Separation Systems," *J. Membrane Sci., 151*, 55–62 (1998).

21. T. K. Poddar and K. K. Sirkar, "A Hybrid of Vapor Permeation and Membrane Based Absorption-Stripping for VOC Removal and Recovery from Gaseous Phase Emissions," *Ibid., 132*, 229–233 (1997).
22. R.-J. Cranford, D. Darmstadt, J. Yang, and C. Roy, "Polyetherimide/Polyvinylpyrrolidone Vapor Permeation Membranes, Physical and Chemical Characterization," *Ibid., 155*, 231–240 (1999).
23. C. K. Yeom and K.-H. Lee, "Vapor Permeation of Ethanol–Water Mixtures Using Sodium Alginate Membranes with Crosslinking Gradient Structure," *Ibid., 135*, 225 (1997).

Received by editor January 26, 1999
Revision received February 2000